Phys. Status Solidi B **249,** No. 6, 1218–1223 (2012) / **DOI** 10.1002/pssb.201100543

physica status solidi b
www.pss-b.com
basic solid state physics

Electron scattering by random adsorbates: A tunable decoherence mechanism in surface bands

Sanjin Marion and Branko Gumhalter*

Institute of Physics, 10000 Zagreb, Croatia

Received 7 September 2011, revised 12 October 2011, accepted 27 October 2011
Published online 27 February 2012

Keywords electron scattering, photoemission spectroscopy, photoexcitation, quasiparticles, surface bands

* Corresponding author: e-mail branko@ifs.hr, Phone: +385 1 4698 805, Fax: +385 1 4698 889

Mechanisms of electron decoherence at surfaces are manifold as they may originate from the various complex interactions of electrons with the static crystal structure and dynamical degrees of freedom of the environment. Decoherence effects manifest themselves in the spectroscopic data in a convoluted fashion and it is usually hard or even impossible to fully disentangle them from each other because of the lack of control of underlying mechanisms by the external observer. However, electronic propagation in quasi-two-dimensional image potential bands (IS-bands) on flat low index surfaces of some metals is subject to an efficient decoherence mechanism that can be controlled externally by careful preparation of the surface. By dosing the concentration (i.e. the coverage) of adsorbates on clean surfaces, which act as randomly distributed scattering centres, one can tune the strength of incoherent IS-electron scattering from defects. Such processes in IS-bands on Cu(100) surface have been investigated by two-photon-photoemission (2PPE) spectroscopy and interpreted using Fermi golden rule approach to calculation of the quasiparticle decay rates and scattering cross sections. However, these results could reproduce the experimental data only in a limited energy interval. Here, we employ the description of electron decoherence in IS-bands based on the propagator approach and infrared renormalization of quasiparticle self-energy and demonstrate that it gives a very good agreement between the theoretical and experimental results for the cross sections. This enables us to discuss the temporal stages of electron dynamics and decoherence in the intermediate states of 2PPE spectroscopy of surface bands.

1 Introduction Owing to the versatility of application modes and high resolution in the energy and time domain the two-photon photoemission (2PPE) spectroscopy has emerged as one of the most powerful tools for the investigation of the electronic structure of gas phase and condensed matter systems. In the past two decades, the applications of 2PPE to solids have provided valuable information on electron dynamics and energetics at surfaces and interfaces [1–4]. In 2PPE spectroscopy of surface bands, the first laser pulse (pump pulse) excites an electron from an initial occupied state below the Fermi energy E_F into an unoccupied image potential state below the vacuum level E_V. The population and dynamics of this intermediate excited electron state is then probed by the second pulse, which lifts the electron to a state above E_V where its energy and momentum $\mathbf{K}$ parallel to the surface are measured. Thereby one obtains information on the properties of the occupied and unoccupied electron states of the system in a single experiment, *albeit* in a convoluted fashion. The results of measurements are commonly interpreted in the quasiparticle picture in which the electron amplitude in the intermediate 2PPE state is expressed as

$$A_{\mathbf{K}} \sim \mathrm{e}^{-i\tilde{E}_{\mathbf{K}}t-\Gamma_{\mathbf{K}}t}, \tag{1}$$

where $\tilde{E}_{\mathbf{K}}$ and $\Gamma_{\mathbf{K}}$ are the quasiparticle effective energy and decay rate, respectively. The deviations from the exponential decay of quantum states has been experimentally evidenced [5–7], although not yet in condensed matter systems. In this work, we shall investigate the applicability of and anticipated deviations from the representation (1) in ultrafast experiments on the benchmark example of electron scattering from defects in surface bands.

A sequence of 2PPE studies of electron scattering from adsorbates in image potential bands on Cu(100) [8–11] have revealed the effect of defects on hot electron dynamics in quasi-two-dimensional (Q2D) states. Quite generally, since the momentum $\mathbf{K}$ is conserved in optical transitions, the electron and hole excited in the first step of a 2PPE process start to propagate coherently with opposite momenta in the respective bands n and n' (for a review of the theory of 2PPE see Ref. [12]). Their subsequent motion is perturbed and decohered by the interactions with defects and dynamical degrees of freedom of the system [13–25]. To assess the effect of localized scatterers on electron propagation in image potential band states (IS states) during the intermediate stage of a 2PPE experiment, we resort to the survival probability approach for decription of decoherence and dephasing processes [21]. This approach is here justified by the fact that the formation of image potential and the corresponding bands on Cu surface proceeds on the ultrashort time scale of $\sim$2 fs upon primary electron excitation of similar temporal spread (cf. Figs. 3 and 5 in Ref. [25]). The survival probability of the quasiparticle state is defined by the relation

$$L_{\mathbf{K},n}(t) = |\langle\psi_{\mathbf{K},n}(0)|\psi_{\mathbf{K},n}(t)\rangle|^2 = |iG_{\mathbf{K},n}(t)|^2, \tag{2}$$

where $\psi_{\mathbf{K},n}(0)$ and $\psi_{\mathbf{K},n}(t)$ are the quasiparticle wavefunctions in the n-th Q2D surface band at the instants $t=0$ and $t>0$, respectively, and $iG_{\mathbf{K},n}(t) = A_{\mathbf{K},n}(t)$ denotes the (retarded) quasiparticle propagator or the Green's function. The latter describes electron evolution in the state $|\mathbf{K},n\rangle$ from the instant of preparation $t=0$ to the instant of detection t, i.e. between the quantum mechanical events of optical excitations induced by the pump and probe photons (cf. Fig. 1 in Ref. [21]). Complementary information is contained in the quasiparticle phase

$$\phi_{\mathbf{K},n}(t) = -\mathrm{Im}\ln[iG_{\mathbf{K},n}(t)]. \tag{3}$$

which together with (2) provides a convenient quantum-mechanical framework for studying the temporal stages of quasiparticle dynamics in the intermediate states of 2PPE from surface bands. In this work, we focus on the theoretical interpretation of selected experimental results reported in Refs. [8–11] using the propagator formalism adapted to the studies of electron scattering by localized defects [26].

2 General properties of quasiparticle dynamics in surface bands The formalism for calculation of $G_{\mathbf{K},n}(t)$ which describes electron scattering from low concentration of random defects in the Q2D image potential bands on metal surfaces was described in detail in Section II of Ref. [17]. The point of departure is the calculation of quasiparticle self-energy $\Sigma_{\mathbf{K},n}(\omega) = \Lambda_{\mathbf{K},n}(\omega) - i\Gamma_{\mathbf{K},n}(\omega)$ that describes electron scattering by randomly distributed impurity potentials V associated with adsorbates. Once $\Sigma_{\mathbf{K},n}(\omega)$ is known, the quasiparticle spectrum $S_{\mathbf{K},n}(\omega)$ is calculated from the standard expression

$$S_{\mathbf{K},n}(\omega) = \frac{\Gamma_{\mathbf{K},n}(\omega)/\pi}{(\omega - E_{\mathbf{K}} - \Lambda_{\mathbf{K},n}(\omega))^2 + \Gamma_{\mathbf{K},n}(\omega)^2}, \tag{4}$$

where $E_{\mathbf{K}}$ is the unperturbed electron energy in the state $|\mathbf{K},n\rangle$. Fourier transform of the spectrum yields the desired Green's function

$$G_{\mathbf{K},n}(t) = -i\Theta(t)\int_{-\infty}^{\infty} \mathrm{d}\omega\, \mathrm{e}^{-i\omega t} S_{\mathbf{K},n}(\omega), \tag{5}$$

which enables calculations of the quasiparticle survival probability (2) and associated phase (3).

Analyses of the general properties of $L_{\mathbf{K},n}(t)$ based on expressions (2)–(5) reveal three distinct temporal stages of quasiparticle propagation affected by the scattering from isolated and randomly distributed adsorbates [17]. For the potentials V that render finite first and second moments of the spectrum (4) the short time propagation amplitude $iG_{\mathbf{K},n}(t)$ can be assessed by time dependent perturbation theory [27, 28]. Under these conditions, the primary stage of quasiparticle propagation before the establishment of energy conservation is ballistic, meaning that external static or dynamic perturbations have a weak effect on the survival probability of the state $|\mathbf{K},\ \mathrm{IS}\rangle$ into which the quasiparticle was initially excited (prepared) by the pump pulse. In this early propagation interval

$$\lim_{t\to 0} L_{\mathbf{K},n}(t) \propto 1 - \left(\frac{t}{\tau_Z}\right)^2, \tag{6}$$

where τ_Z is the so-called Zeno time [28] characterizing the quasiparticle amplitude reduction during early ballistic motion. τ_Z is a $\mathbf{K}$-independent off-the-energy-shell quantity that depends only on the gross properties of quasiparticle spectrum [17].

In the second stage that corresponds to longer propagation times, the energy conservation sets in and the standard quasiparticle picture can be applied to describe the motion of electrons promoted into the band states. Here, the amplitude of the excited particle perturbed by random defects is of the form (1), i.e. it is characterized by a quasistationary phase comprising the renormalized quasiparticle energy $\tilde{E}_{\mathbf{K}} = E_{\mathbf{K}} + \Lambda_{\mathbf{K}}(E_{\mathbf{K}})$ and decay rate $\Gamma_{\mathbf{K}} = \Gamma_{\mathbf{K}}(\tilde{E}_{\mathbf{K}})$. Hence, in this interval

$$L_{\mathbf{K},n}(t) \propto \mathrm{e}^{-2\Gamma_{\mathbf{K}}t}, \tag{7}$$

where for low concentration c of adsorbates one finds $\Gamma_{\mathbf{K}} \propto c$. It is precisely this interval of propagation past the initial ballistic stage (6), which allows one to introduce the notion of quasiparticle lifetime $\tau_{\mathbf{K}} = 1/2\Gamma_{\mathbf{K}}$. The quasistationary regime also enables the definition of total cross section per adsorbate for electron scattering from a random array of adsorbates through the relation

$$\sigma_{\mathbf{K}} = \frac{2\Gamma_{\mathbf{K}}}{cj_{\mathbf{K}}}, \tag{8}$$

where $j_{\mathbf{K}} = K/m_e$ is the electron current in the state $|\mathbf{K}\rangle$. In Ref. [9] the values of $\Gamma_{\mathbf{K}}$ and the corresponding $\sigma_{\mathbf{K}}$ were first determined from 2PPE measurements and then calculated for intraband electron scattering by the dipole potential of adsorbates using Fermi's golden rule (FGR). This calculation corresponds to the second order perturbation theory or Born approximation (BA) treatment of electron scattering by isolated impurities whose validity will be critically examined in Section 3.

The duration of quasiparticle decay described by the exponential law (7), designated the quasiparticle lifespan, may exceed the lifetime $\tau_{\mathbf{K}}$ by several orders of magnitude till the destructive interference of the amplitudes arising from different components of the spectrum (4) cause the wavefunction collapse [29, 27]. Past the collapse, in the third asymptotic stage of propagation, the particle survival probability in Q2D bands perturbed by random point defects follows the behaviour

$$\lim_{t\to\infty} L_{\mathbf{K},n}(t) \propto \frac{1}{t^2\,(\ln t)^4}, \tag{9}$$

which is a much slower decay than in the intermediate stage described by (7). In the following, we shall present a quantitative analysis and discussion of the processes described qualitatively by expressions (6)–(9) for the case of dipolar electron–adsorbate scattering in the first IS-band on Cu(100) surface ($n = 1$) and bring them in contact with the experimental results reported in Ref. [9].

3 Model calculations of quasiparticle dynamics

The parameters controlling the magnitudes of τ_Z, $\tau_{\mathbf{K}}$ and $\sigma_{\mathbf{K}}$, as well as of the overall durations of the three above discussed propagation intervals, are the strength of the interaction V governing the electron–adsorbate scattering in the IS-band, the concentration c or the coverage Θ of randomly distributed adsorbates, and the (quasi)dimensionality of the IS-bands. In Section II of Ref. [17], we presented detailed derivations of the survival probabilities leading to expressions (6)–(9). Assuming that V arises from hot electron interaction with static adsorbate dipoles [9] one can obtain Dyson's expansion for the leading component of self-energy that is linear in adsorbate concentration c. The lowest order diagrams of this series in the perturbation V are shown in Fig. 1.

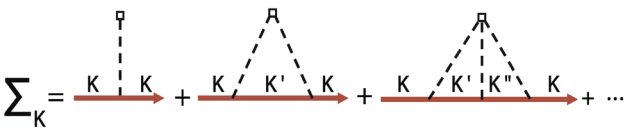

Figure 1 (online colour at: www.pss-b.com) Lowest-order self-energy diagrams which are linear in the concentration of adsorbates. Full lines symbolize electron propagators and dashed lines the adsorbate scattering potential centered at the same site (denoted by small vertex quadrangle).

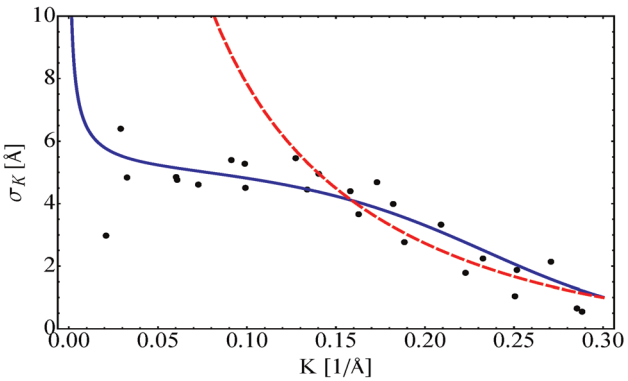

Figure 2 (online colour at: www.pss-b.com) Total cross section $\sigma_{\mathbf{K}}$ for scattering of electrons from Cu adatoms in the first image potential band on Cu(100). Experimental points [9] denoted by dots. Dashed line: $\sigma_{\mathbf{K}}^{(2)}$ calculated from FGR expression with electron–adsorbate potential from Ref. [9] and concentration corresponding to adsorbate coverage $\Theta = 0.7\%$. Full line: Same quantity after renormalization described in the text.

Approximate expressions for $\Sigma_{\mathbf{K}}(\omega)$ that can be brought in direct comparison with the calculations of cross sections reported in Ref. [9] assume weak electron–adsorbate interaction V. The weak coupling condition ensures fast convergence of the series for the self-energy and its approximate representation by the first two diagrams depicted in Fig. 1 which yield $\Sigma_{\mathbf{K}}^{(2)}(\omega) = \Lambda_{\mathbf{K}}^{(2)}(\omega) - i\Gamma_{\mathbf{K}}^{(2)}(\omega)$. This approximaton leads to the FGR or BA expression for $\Gamma_{\mathbf{K}}^{(2)}$ which is equal to the one used in Ref. [9]. In Fig. 2, we show by the dashed line the corresponding BA cross section $\sigma_{\mathbf{K}}^{(2)}$ obtained using (8) for IS-electron scattering from Cu adatoms on Cu(100) surface and compare it with the experimental data [9]. Note that by construction these values of $\sigma_{\mathbf{K}}^{(2)}$ are identical to the ones shown in Fig. 6 of Ref. [9]. Variation of the components of $\Sigma_{\mathbf{K}}^{(2)}(\omega)$ and the IS-electron spectrum calculated thereof are shown in Figs. 3 and 4, respectively, as dashed lines. Likewise, the IS-electron survival probability calculated in the same approximation and illustrating the three quasiparticle propagation stages typified by expressions (6), (7) and (9) is shown as dashed line in Fig. 5.

The agreement between the experimental and the BA or FGR-derived values for $\sigma_{\mathbf{K}}^{(2)}$ shown in Fig. 2 is fairly good for electron wavevectors $K > 0.15$ Å^{-1}. However, it is much less satisfactory in the infrared region near the band bottom even if the relatively large experimental error in that interval is included (cf. Fig. 6 of Ref. [9]). Hence, all the results derived from approximate $\Sigma_{\mathbf{K}}^{(2)}(\omega)$ require special attention regarding their reliability in the infrared region where $\sigma_{\mathbf{K}}^{(2)}$ fails to reproduce the experimental data.

In the following, we explore the origin of and suggest the procedure to remedy this limitation of the FGR approach in the application to electron–adsorbate potential scattering. To investigate the possible sources of this variance, we recall from Ref. [17] that due to a combined effect of the form of

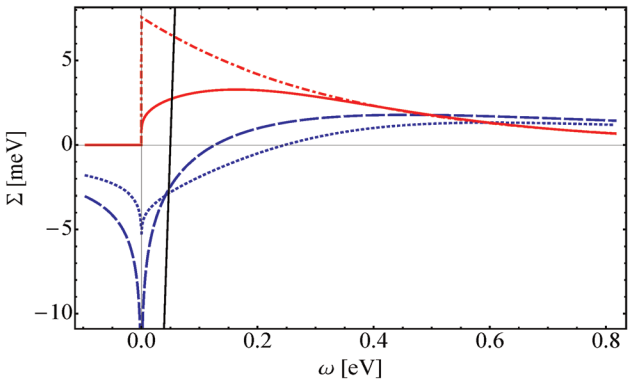

Figure 3 (online colour at: www.pss-b.com) Comparison of the real and imaginary parts of the quasiparticle self-energy as calculated within the FGR approach and from the fully renormalized self-energy in the equivalent pseudopotential approach. Dash-dotted line: $\Gamma^{(2)}_{\mathbf{K}}(\omega)$, long dashed line: $\Lambda^{(2)}_{\mathbf{K}}(\omega)$, full line: $\Gamma_{\mathbf{K}}(\omega)$, dotted line: $\Lambda_{\mathbf{K}}(\omega)$. Intersection of the steep line $\omega - E_{\mathbf{K}}$ for $E_{\mathbf{K}} = 50$ meV ($K = 0.115$ Å^{-1}) with $\Lambda_{\mathbf{K}}(\omega)$ giving the position of spectral maximum in Fig. 4.

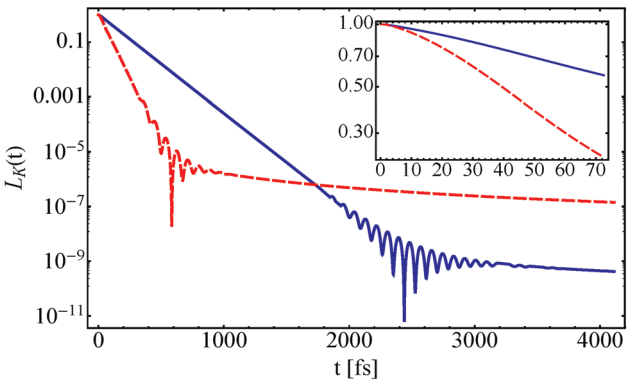

Figure 5 (online colour at: www.pss-b.com) Survival probability $L_{\mathbf{K}}(t)$ of the photoexcited electron initial state $|\mathbf{K}, n = \mathrm{IS}\rangle$ as a function of time for initial energy $E_{\mathbf{K}} = 50$ meV ($K = 0.115$ Å^{-1}). Dashed line: $L_{\mathbf{K}}(t)$ calculated with the self-energy approximated by the first two terms in Fig. 1. Full line: same quantity after infrared renormalization described in the text. Note logarithmic scale on the vertical axis. Inset shows the early Zeno behaviour (6). Renormalization shifts the wavefunction collapse from ~600 fs to ~2400 fs.

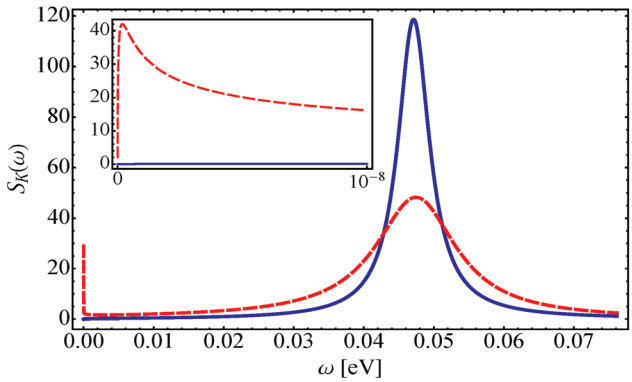

Figure 4 (online colour at: www.pss-b.com) Comparison of the IS-electron spectra calculated with approximate $\Sigma^{(2)}_{\mathbf{K}}(\omega)$ (dashed line) and infrared renormalized $\Sigma_{\mathbf{K}}(\omega)$ (full line). Initial electron energy $E_{\mathbf{K}} = 50$ meV ($K = 0.115$ Å^{-1}). Renormalized spectrum is dominated by Lorentzian-like quasiparticle peak whose position is determined by the zero of expression $(\omega - E_{\mathbf{K}} - \Lambda_{\mathbf{K}}(\omega))$ outside the infrared region.

scattering matrix elements $V_{\mathbf{K},\mathbf{K}'}$ and the Q2D character of the IS-band, the approximate self-energy $\Sigma^{(2)}_{\mathbf{K}}(\omega)$ exhibits a logarithmic divergence in a narow region of quasiparticle energies near the band bottom which produces a threshold hump in $S^{(2)}_{\mathbf{K}}(\omega)$ (see inset in Fig. 4). Hence, the truncation of the series for $\Sigma_{\mathbf{K}}(\omega)$ and its approximation by $\Sigma^{(2)}_{\mathbf{K}}(\omega)$ may no longer be justified in this region of the quasiparticle spectrum irrespective of the weakness of the interaction V (i.e. the smallness of the expansion parameter). Therefore, to obtain consistent results for $\Sigma_{\mathbf{K}}(\omega)$ near the band bottom, and thereby of $S_{\mathbf{K}}(\omega)$ and $\sigma_{\mathbf{K}}$, all the logarithmically divergent contributions from the series in Fig. 1 should be taken into account.

The problem of proper treatment of the logarithmically divergent self-energy and vertex corrections near the excitation thresholds, usually termed the infrared renormalization, is common in the studies of electron interactions with localized perturbations [30–32]. In the present work, we shall adopt some technical aspects used in these procedures. To this end, we note that for quasiparticle states near the band bottom (i.e. for small K) the associated De Broglie wavelengths may largely exceed the range of electron–adsorbate interactions. This suggests an approximate treatment of the series for $\Sigma_{\mathbf{K}}(\omega)$ in which the dipolar potential V is replaced by a contact pseudopotential whose strength is adjusted to yield equivalent values of the renormalized $\sigma_{\mathbf{K}}$ and the FGR-derived $\sigma^{(2)}_{\mathbf{K}}$ in the energy interval where FGR reproduces well the experimental results. In the present problem, this applies to the data for which $K > 0.15$ Å^{-1} [9]. The substitution of contact pseudopotential matrix elements in the expressions for Feynman diagrams constituting $\Sigma_{\mathbf{K}}(\omega)$ and depicted in Fig. 1 leads to an infinite geometric series in powers of logarithmically divergent terms that are all linear in c and can be easily summed up. This procedure strongly renormalizes $\Sigma_{\mathbf{K}}(\omega)$ in the infrared region $\omega \to 0$ but has negligible effect at higher energies. Thereby the consistency of adjustment of the pseudopotential strength for large K, or the equivalence of the scattering phase shifts, is preserved. Substitution of the thus obtained imaginary part of the on-the-energy-shell self-energy in (8) yields the infrared renormalized scattering cross section $\sigma_{\mathbf{K}}$ whose variation with K is shown in Fig. 2 by a full line. The almost perfect agreement of such renormalized $\sigma_{\mathbf{K}}$ with the experimental data over a broad range of quasiparticle momenta, and particularly in the critical low-K limit, signifies the importance of taking into account singular multiple scattering processes through infrared renormalization of the

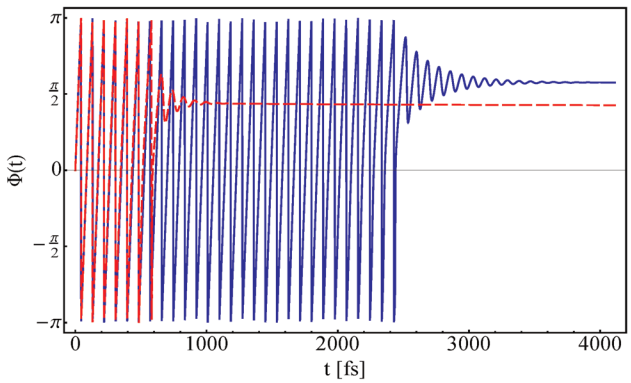

Figure 6 (online colour at: www.pss-b.com) Phase $\phi_{\mathbf{K}}(t)$ (modulo 2π) of the photoexcited IS-electron for initial energy $E_{\mathbf{K}} = 50$ meV ($K = 0.115$ Å^{-1}). $\phi_{\mathbf{K}}(t)$ calculated with the self-energy approximated by the first two terms in Fig. 1. Full line: same quantity after infrared renormalization. Note that the phase collapses simultaneously with the corresponding survival probability shown in Fig. 5.

contributions to the quasiparticle self-energy that have here been carried out on the terms linear in c. The remaining spurious steep uprise of calculated $\sigma_{\mathbf{K}}$ for $K < 0.02$ Å in Fig. 2 could be healed (softened) by carrying out infrared renormalization of the self-energy by going beyond the present approximations, viz. restriction to the terms linear in concentration and the use of contact pseudopotential. However, the large experimental error incurred in this region (cf. Fig. 6 in Ref. [9]) does not warrant the huge increase of computational effort required to yield the data for comparison with measurements.

Renormalization of the second order self-energy also implies renormalization of the quasiparticle spectrum $S^{(2)}_{\mathbf{K}}(\omega)$ in the same domain. The resulting effect on the quasiparticle dynamics is twofold: (i) the spectral intensity near the band bottom (excitation threshold) is diminished, leading to the enhancement of quasiparticle lifespan in which the standard quasiparticle picture (1) holds, and (ii) the width of quasiparticle peak at $E_{\mathbf{K}}$ is reduced, leading to a longer lifetime within the quasiparticle lifespan. These features are illustrated in Figs. 4–6. This should generally favour the observation of standard quasiparticle features (i.e. the well defined energy and lifetime) in TR 2PPE from image potential bands. In the case of lesser importance of other decoherence mechanisms such a simple quasiparticle evolution would occur in the interval of pump–probe delays between ∼20 and ∼2000 fs which is free from early or asymptotic transients that produce non-stationary behaviour of the type (6) and (9), respectively. In turn, this facilitates the use of optical Bloch equations involving the standard form of decay matrices [21] $\hat{\mathbf{\Gamma}}$ for the interpretation of experimental data in the same evolution interval. Conversely, the presence of transients leading to the non-stationary (non-exponetial) evolution and decay [19–21, 25] prevents simple modelling of the quasiparticle decoherence in terms of phenomenologically parametrized $\hat{\mathbf{\Gamma}}$ and the ensuing Bloch equations. Although these findings have been quantified for the high quality data available only for the Cu(100) surface, and in this sense are system specific, their general validity should hold for other surface bands perturbed by similar effective defect potentials. In particular, the dynamics of holes excited in the occupied parts of surface state bands on Cu(111) and Ag(111) faces may exhibit analogous behaviour but the experimental evidence of such phenomena is still lacking. With improving resolution of photoemission experiments the likelyhood of observation of non-exponential decay of quasiparticles in surface bands would probably be least critical in the early stage of propagation during which the amplitude signal may still be strong enough, likewise in some paradigmatic systems studied earlier [33].

Acknowledgements This work has been supported in part by the Ministry of Science, Education and Sports of the Republic of Croatia through the Research Project No. 035-0352828-2839.

References

[1] R. Haight, Surf. Sci. Rep. **21**, 275 (1995).
[2] E. Bertel, Surf. Sci. **331**, 1136 (1995).
[3] T. Fauster and W. Steinmann, in: Electromagnetic Waves: Recent Developments in Research, Vol. 2, P. Halevi (ed.) (North Holland, Amsterdam, 1995), p. 347.
[4] H. Petek and S. Ogawa, Prog. Surf. Sci. **56**, 239 (1997).
[5] A. Peres, Ann. Phys. (New York) **129**, 33 (1980). and references therein.
[6] S. R. Wilkinson, C. F. Bharucha, M. C. Fischer, K. W. Madison, P. R. Morrow, Q. Niu, B. Sundaran, and M. G. Raizen, Nature **387**, 576 (1997).
[7] C. Rothe, S. I. Hintschich, and A. P. Monkman, Phys. Rev. Lett. **96**, 163601 (2006).
[8] K. Boger, M. Weinelt, and Th. Fauster, Phys. Rev. Lett. **92**, 126803 (2004).
[9] K. Boger, Th. Fauster, and M. Weinelt, N. J. Phys. **7**, 110 (2005).
[10] M. Hirschmann and Th. Fauster, Appl. Phys. A **88**, 547 (2007).
[11] Th. Fauster, M. Weinelt, and U. Höfer, Prog. Surf. Sci. **82**, 224 (2007).
[12] H. Ueba and B. Gumhalter, Prog. Surf. Sci. **82**, 193 (2007).
[13] A. G. Borisov, A. K. Kazansky, and J. P. Gauyacq, Phys. Rev. B **65**, 205414 (2002).
[14] F. E. Olsson, A. G. Borisov, M. Persson, N. Lorente, A. K. Kazansky, and J. P. Gauyacq, Phys. Rev. B **70**, 205417 (2004).
[15] A. G. Borisov, J. P. Gauyacq, and A. K. Kazansky, Surf. Sci. **540**, 407 (2003).
[16] F. E. Olsson, A. G. Borisov, and J. P. Gauyacq, Surf. Sci. **600**, 2184 (2006).
[17] B. Gumhalter, A. Šiber, H. Buljan, and Th. Fauster, Phys. Rev. B **78**, 155410 (2008).
[18] F. El-Shaer and B. Gumhalter, Phys. Rev. Lett. **93**, 236804 (2004).
[19] P. Lazić, V. M. Silkin, E. V. Chulkov, P. M. Echenique, and B. Gumhalter, Phys. Rev. Lett. **97**, 086801 (2006).
[20] P. Lazić, V. M. Silkin, E. V. Chulkov, P. M. Echenique, and B. Gumhalter, Phys. Rev. B **76**, 045420 (2007).
[21] P. Lazić, D. Aumiler, and B. Gumhalter, Surf. Sci. **603**, 1571 (2009).

[22] P. M. Echenique, J. M. Pitarke, E. V. Chulkov, and A. Rubio, Chem. Phys. **251**, 1 (2000).
[23] P. M. Echenique, R. Berndt, E. V. Chulkov, Th. Fauster, A. Goldman, and U. Höfer, Surf. Sci. Rep. **52**, 219 (2004).
[24] E. V. Chulkov, A. G. Borisov, J. P. Gauyacq, D. Sánchez-Portal, V. M. Silkin, V. P. Zhukov, and P. M. Echenique, Chem. Rev. **106**, 4160 (2006).
[25] B. Gumhalter, P. Lazić, and N. Došlić, Phys. Status Solidi B **247**, 1907 (2010).
[26] S. Doniach and E. H. Sondheimer, Green's Functions for Solid State Physicists (W.A. Benjamin, Inc., Reading, Massachusets, 1974), Chap. 5.
[27] E. Rufeil Fiori and H. M. Pastawski, Chem. Phys. Lett. **420**, 35 (2006).
[28] P. Facchi and S. Pascazio, J. Phys. A, Math. Theor. **41**, 493001 (2008).
[29] L. Khalfin, Sov. Phys. JETP **6**, 1053 (1958).
[30] P. W. Anderson, Phys. Rev. Lett. **18**, 1049 (1967).
[31] G. D. Mahan, Phys. Rev. **163**, 612 (1967).
[32] P. Nozières and C. T. De Dominicis, Phys. Rev. **178**, 1097 (1969).
[33] For a list of references on observation of early non-exponential decay of quantum states see Section 1.2. in Ref. [28].